

PROTECTION PERFORMANCE ASSESMENT WITH GRID FORMING CONVERTER ACTING AS A REFERENCE GENRATOR DURING BLACK START

Eleni Tsotsopoulou^{*1}, *Dimitrios Tzelepis*¹, *Agusti Egea*¹, *Neil Miller*², *Adam Dysko*¹

¹*Department of Electronic and Electrical Engineering, University of Strathclyde, Glasgow, United Kingdom*

²*SP Energy Networks, Glasgow, UK*

**eleni.tsotsopoulou.2018@uni.strath.ac.uk*

Keywords: GRID-FORMING CONVERTER, BLACK-START, OVERCURRENT PROTECTION

Abstract

The studies presented in this paper aim to assess the operation of existing protective schemes (i.e. overcurrent protection) within UK networks, considering black-start scenario initiated from converter-based distributed energy sources. The primary objective is to investigate whether it is realistically feasible for a converter-based battery storage unit, to replace a synchronous generator in black-start scenarios, and deliver the same benefits accounting for adequate fault levels and reliable protection operation. The case studies include transmission and distribution level (11kV up to 400kV) fault level calculations and assessment of the protection performance under balanced/unbalanced faults considering existing settings proposed for such black-start conditions. Furthermore, the utilization of a voltage-controlled overcurrent protection scheme is investigated as a potential protection solution, to address the reduced fault levels resulting from the converter-based source. The results and observations aim to build a solid foundation for the design of protection schemes during black-start scenarios within distribution systems.

1 Introduction

Traditionally, black-start services are provided by large Synchronous Generators (SGs) which meet all the technical requirements to operate as reference generators. The term reference generator signifies the generation unit which is utilized to restore the system after a blackout event and must be capable of providing voltage and frequency regulation, enabling the connection of additional generation units, ensuring the connection of demand and facilitating the energization of the wider network where possible [1]. From the protection operation perspective, the high fault current provided naturally by the SGs, ensures adequate protection operation, and subsequently enables secure restoration of the wider grid.

In an attempt to remove the total dependence on large and costly SGs, the need for greater generation diversity in black-start services has emerged. Responding to the significant changes in energy landscape, several studies and research projects envisage how the Distributed Energy Resources (DERs) can participate in black-start services [2][3][4]. However, the creation of self-sustained power islands with high penetration of DERs, creates significant system issues which may lead to certain risks that need to be managed. One of the most important challenges is associated with the reduced fault levels which affect the sensitivity of the existing protection schemes (i.e. over-current protection) and the protection coordination, potentially jeopardizing the restoration process.

The studies presented in this paper aim to investigate the over-current protection limitations and the required changes with respect to the protection settings, to facilitate the adoption of a Grid-Forming Converter (GFC) unit as a reference generator

in black-start scenarios. In particular, the reported studies aim to assess the performance of the existing over-current protection devices when the main SG reference unit has been replaced by a GFC unit of equal size, driven by a battery storage system, within UK SP Distribution (SPD) and SP Transmission (SPT) networks. The deployment of the SG as reference generator has been considered for benchmarking purposes. The ultimate goal is to provide observations to benefit the design of future black-start protection schemes within the distribution systems and propose alternative protection solutions.

2 Examined Power System

The studies conducted in this paper are based on a replica model of the SPEN network in the vicinity of the Chapelcross 132/33kV grid supply point (GSP), located in southwest Scotland. The model has been developed by SPEN in DiGSILENT PowerFactory software. An overview of the substations in the Chapelcross area and the substation interconnections are depicted in Figure 1. The system incorporates voltage levels from 415 V to 400 kV. The reference generator is connected at the Chapelcross 33kV busbar via a 53 MVA transformer, for the case of the SG and 61 MVA for the case of the GFC unit, earthed on the 33 kV side. Two generating units were considered as reference generators: an SG (with export net capacity of 45 MW) which was utilised to obtain a benchmark case study, and similarly-sized (i.e. 60 MVA/ 45 MW size) GFC unit to replace the SG.

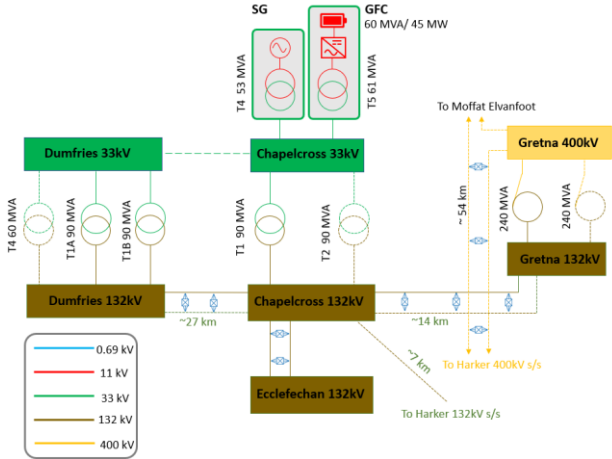


Figure 1: Test network at Chapelcross GSP area.

The GFC unit is composed of three main components: i) a lithium-ion 13 Ah battery, ii) a 60 MVA converter and iii) a step-up transformer.

3 Fault response of Grid-forming unit

A variety of GFC control strategies have been proposed in the literature such as droop [5], multi-droop [6] and virtual synchronous machine [7], to name a few. The main objective of all the control strategies is to force the GFC unit to operate as an independent controllable voltage source. GFC units control active and reactive power, by directly adjusting the voltage angle and magnitude (without a requirement for a synchronisation loop, i.e. PLL). Hence, GFC units exhibit black-start capability by providing voltage and frequency support within the islanded system.

In the presented fault analysis studies two main aspects of the GFC unit have been considered:

- i) fast-acting voltage support as a useful feature for sustaining high fault currents, and
- ii) the saturated output current (i.e. the current output which the converter generates after it has reached its rated output and reverted to current injection mode).

During the balanced and unbalanced faults in the islanded system, GFC unit regulates its output current to provide voltage support. The magnitude of the current is adjusted by the voltage controller which targets the nominal voltage at the HV side of the transformer. This voltage support is subject to current limitation threshold imposed by the current control loop. However, during any transient event which can lead to a dramatic decrease in the retained voltage (such as the close-up faults), the injected current is higher to enhance the voltage profile. Under these conditions, the value of the current reaches the maximum current of the GFC (current limitation threshold) and the GFC is saturated. The inclusion of the current saturation forces the GFC unit to switch to current injection control mode and behaves as a constant current source. In this work, the current limitation threshold has been set to 1.05 p.u. (base current is the GFC nominal current). Once this threshold has been reached during the faults, the

GFC unit is saturated and locked to inject continuously 1 p.u current.

To obtain a better insight into the GFC's fault response, the RMS simulation studies were conducted in DigSILENT PowerFactory for two 3-Phase (LLL) faults (F_1, F_2) applied at two different 33 kV busbars within the tested network (as indicated in Figure 2).

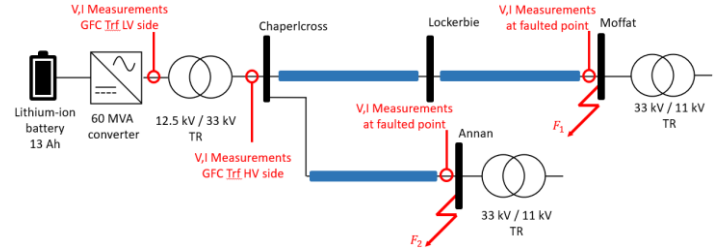


Figure 2: Fragment of the test network (33 kV).

In both scenarios the fault occurred at $t = 1$ s, and the simulated RMS traces include: i) the current and voltage on the HV side of the GFC's transformer (33kV), ii) the current and voltage on the LV side of the GFC's transformer (12.3 kV), and iii) the current at the fault point. The simulated RMS waveforms are shown in Figures 3 to Figure 5

Figure 3 and Figure 4 present the response of the GFC during the simulation studies for the two selected faults at 33kV busbars, while Figure 5 illustrates the resulting fault currents at the faulted points. As can be seen in Figure 3(c), for a LLL fault at Moffat 33 kV busbar, the voltage at the HV side of the GFC transformer is depressed but is sustained above the 90% of the nominal value. In this case, the reactive current provided by the GFC to support voltage does not exceed the maximum current limit. Particularly, on the HV and LV side of the GFC transformer, the injected current is only 0.65 p.u, which does not cause the GFC saturation, and the converter continues to behave as a voltage source. At the fault point the current is approximately 0.75 p.u. (Figure 5 (a)).

Conversely, for an LLL fault at Annan 33kV busbar, the voltage at HV side the GFC transformer is reduced to 0.14 p.u. (Figure 4 (c)), and at LV side the voltage is depressed to 0.3p.u. (Figure 4(d)). The value of the reactive current injected by the GFC unit to support the retained voltage reaches the current limitation threshold, leading to the GFC saturation. It is noticeable from Figure 4(a) and (b) that the GFC has switched to the current control mode and locks its output current to 1 p.u. The current at the fault point is 0.97 p.u. (Figure 5 (b)).

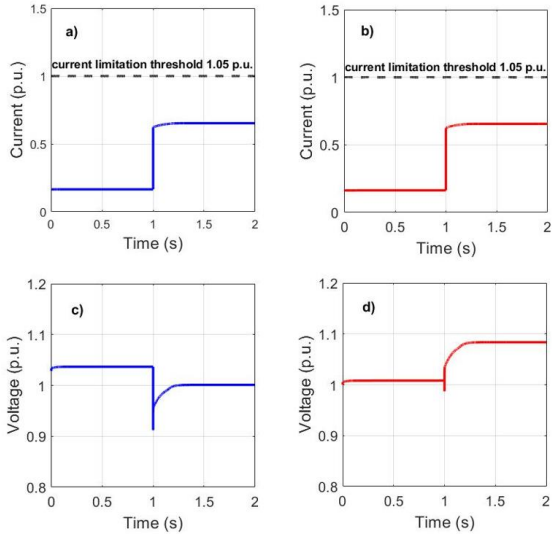


Figure 3: Simulation results for a LLL fault at Moffat 33kV busbar: (a) current at HV of GFC transformer, (b) current at LV side of GFC transformer, (c) voltage at HV side of GFC transformer, (d) voltage at LV side of GFC transformer.

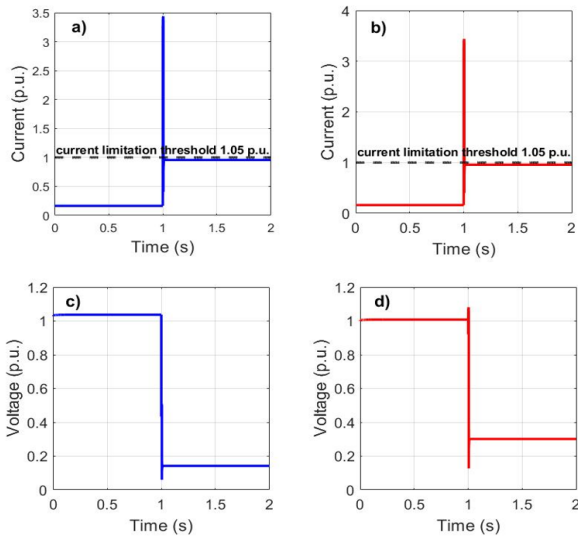


Figure 4: Simulation results for a LLL fault at Annan 33kV busbar: (a) current at HV side of GFC transformer, (b) current at LV side of GFC transformer, (c) voltage at HV side of GFC transformer, (d) voltage at LV side of GFC transformer.

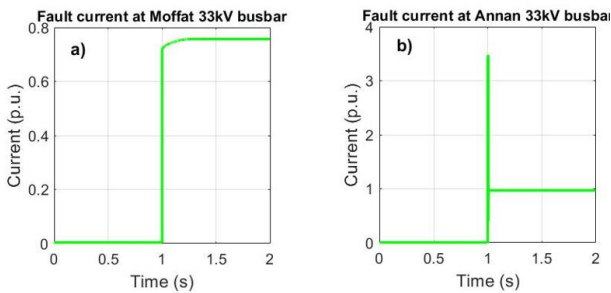


Figure 5: Fault current at the fault point for an LLL fault at: (a) Moffat 33kV busbar (b) Annan 33kV busbar.

4 Fault levels and protection assessment studies

4.1 Fault levels calculations

To quantify the impact of the GFC unit on the system fault levels in black-start conditions, a series of fault level calculations have been conducted across all voltage levels considering first SG, and then GFC unit as reference generator. The main objective of this comparative analysis is to determine whether it is realistically feasible to replace the SG with a GFC unit and still provide adequate fault levels to ensure reliable protection operation during the system's re-energization.

For the fault levels calculation studies the following three distinct cases were examined:

- Case 1 – Static short-circuit analysis and SG as reference generator
- Case 2 – Static short-circuit analysis and GFC as reference generator .
- Case 3 – RMS dynamic short-circuit analysis and GFC as reference generator .

Figure 6 and Figure 7 present the selected results of the fault level analysis conducted for three-phase (LLL) and single-phase-to-ground (LG) faults at different voltage levels. The comparative analysis is based on the magnitude of the fault current flowing 1 s after the fault occurrence (I_k). The results reported here include the fault level calculation method in accordance with the IEC 60909 standard for the case of the SG (bar graph in black), and the GFC unit (bar graph in red). Additionally, for the case of the GFC unit, the fault level contribution has been also calculated using time domain RMS simulation (bar graph in green). The result demonstrates a notable difference between static and RMS based calculations which can more accurately represent the impact of fast acting control features (e.g. voltage regulation), not included in standard (static) fault level analysis.

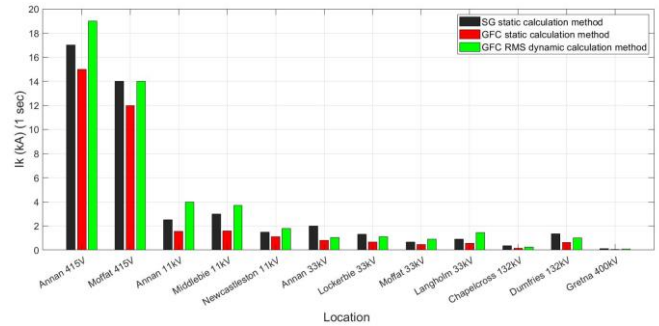


Figure 6: Three-phase fault levels.

It can be observed that the fault levels from the RMS dynamic simulation are generally higher compared to those derived by the static calculation method. This results from the inclusion of the fast-acting voltage regulator in the GFC dynamic model which is not represented in the IEC 60909 calculations.

Furthermore, by comparing the results (for both the LLL and LG faults) resulting from the SG and those provided by the GFC (using the RMS results) it has been revealed that:

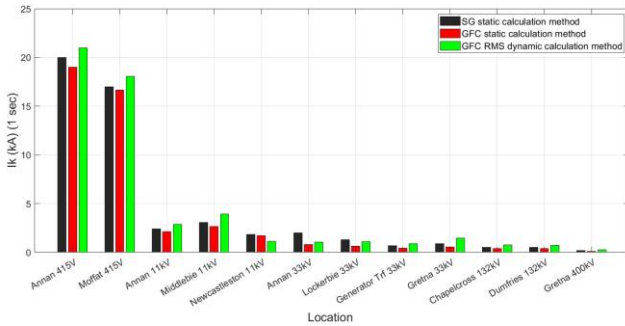


Figure 7: Single-phase-to-ground fault levels.

- At lower voltage levels (11 kV) the LLL and LG fault levels contributed by the GFC, are higher than those of the SG. For these voltage levels, the fast-acting voltage support of the GFC has proven to be a useful feature for sustaining high fault currents.
- At 33kV, when the GFC does not operate in current injection mode (no saturation), it can provide higher LLL and LG fault levels compared to those of the SG. Conversely, for the LLL and LG faults during which the current limitation threshold is reached, the fault current infeed is limited to the value of the nominal current (unless converter is purposefully oversized).
- At 132 kV and 400 kV, the LLL fault levels follow the same trend to those at 33 kV. However, the LG faults do not lead to GFC's saturation, resulting in higher fault levels compared to those provided by the SG.

Based on the key observations drawn by the RMS simulation analysis, it can be inferred that at higher voltage levels (i.e. 33 kV, 132 kV and 400 kV) the GFC is saturated in most cases. Therefore, the resulting fault levels are reduced, affecting the protection operation. Considering this, if it is desirable to energise parts of the network at higher voltage levels during black-start conditions, it is expected that protection modification may be required to enable the adoption of GFC unit as reference generator. Contrarily, at lower voltage levels (i.e. 11 kV) the GFC unit operates satisfactorily as a reference generator providing sufficiently high fault levels. Hence, it is anticipated that protection sensitivity is not compromised.

4.2 Protection assessment studies

To examine the impact of the GFC unit on the performance of the existing protection schemes, LLL and LG fault levels have been calculated for faults applied at all busbars in the examined system (i.e. 11kV, 33kV, 132kV and 400kV), considering the three investigated cases introduced in subsection 4.1.

The principal objective of the protection assessment studies is to determine whether the typical protection settings proposed for black-start conditions considering the SG as reference generator (Case 1), are adequate for the GFC unit (Case 2 and Case 3) [8]. The protection schemes under test, include conventional overcurrent relays tested for LLL faults and overcurrent earth fault relays, tested under LG faults.

Two protection assessment studies are included in this section as an illustration of the applied methodology. Figure 8 and Figure 9 illustrate the overcurrent grading curves for a LLL solid fault at 11 kV Lockerbie busbar and a LLL solid fault occurring at 33 kV transformer incomer to Annan switchboard, respectively.

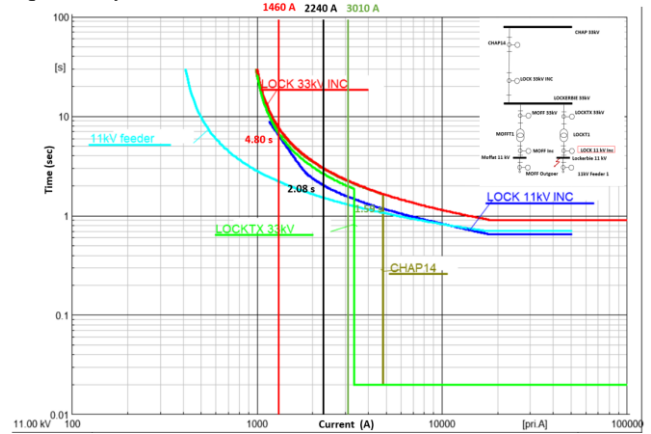


Figure 8: Overcurrent grading curves for LLL fault at 11kV Lockerbie busbar

As it can be seen in Figure 8, the overcurrent relay that must operate first for a LLL at 11 kV Lockerbie busbar is the overcurrent 'LOCK 11kV Inc' relay, installed at 11kV transformer incomer. The fault current contributed by the GFC unit as reference generator and derived from the RMS simulation is 3010 A and is higher compared to the other two cases. Subsequently, for Case 3, the relay operates at 1.59 s and clears the fault 0.49 s faster compared to the Case 1, which considers the SG as reference generator. Regarding Case 2, the resulting fault current is the lowest, leading to the highest fault clearance time (4.80 s).

Nevertheless, it must be pointed out that the time grading between 'LOCK 11kV INC' relay at transformer incomer and '11kV Feeder' relay at 11 kV feeder is reduced and the two characteristics cross each other. Under these conditions the protection discrimination for a LLL fault at 11 kV feeder is jeopardised. Furthermore, the fault current infeed from the GFC unit for a LLL fault at the 11 kV Lockerbie is very close to the instantaneous element of the 'LOCKTX 33kV' relay at 33 kV transformer incomer. Therefore, for a fault at 11 kV during black-start conditions and considering the GFC unit as reference generator, the protection sensitivity is sufficient. The settings proposed for the SG as reference generator [8], are anticipated to operate adequately for any fault at 11 kV busbar in terms of protection sensitivity. However, in some cases, adjustments to the time delay settings are required to enhance protection discrimination.

In Figure 9, the overcurrent relay 'CHAP13' installed at 33 kV side of the transformer, operates at 0.02 s for Case 1, at 2.80 s

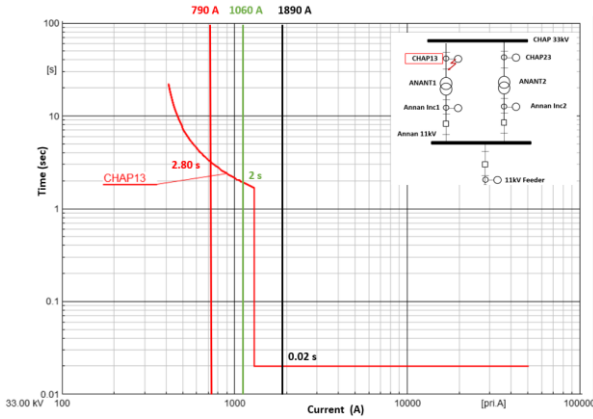


Figure 9: Overcurrent grading curve for LLL solid fault at 33kV transformer incomer to Annan switchboard

for Case 2, and at 2 s for Case 3, respectively. The higher fault clearance time for the cases with the GFC unit as reference generator can be interpreted based on lower resulting fault current infeed. For a LLL solid fault at 33 kV transformer incomer to Annan switchboard, the GFC is saturated, and its fault current infeed obtained from the RMS simulation calculation is reduced to 1060 A and from the static short-circuit analysis it is decreased to 790 A. Therefore, at 33 kV when the GFC reference generator is saturated, more sensitive overcurrent pick-up settings are required to ensure faster fault clearance times.

6 Voltage-controlled protection scheme

This section evaluates the adaptation of voltage-controlled overcurrent protection on the 33 kV transformer incomers, as a potential mitigating protection solution to tackle the adverse effect of the GFC saturation on the protection sensitivity. The key advantage of the voltage-dependent protection is that the overcurrent pick-up setting is automatically reduced when the measured voltage drop at the switchboard is below a pre-defined value. Therefore, more sensitive protection can be attained leading to lower fault clearance time and higher degree of sensitivity.

The arrangement of the developed voltage-dependent relay is illustrated in Figure 10, while Table 1 presents the setting utilized in the protection assessment studies.

Table 1: Settings of voltage-dependent relay.

Settings	Values
Voltage setting	85% of the nominal voltage
IDMT standard setting	Same to those reported in [8]
IDMT sensitive setting	50% of standard setting

The voltage-controlled relay has an undervoltage setting and two overcurrent settings (i.e standard and sensitive setting). The presence of the fault is detected by the undervoltage element. Once the voltage sensed by the voltage measuring elements drops below the 85% of the nominal voltage, the relay is switched to a more sensitive setting (sensitive curve in Figure 10), which at this example, is equal to 50% of the standard pick-up overcurrent setting. The transition to the more sensitive curve reduces the risk of non-detection when the GFC is saturated, and the magnitude of its fault current infeed is below the standard overcurrent setting.

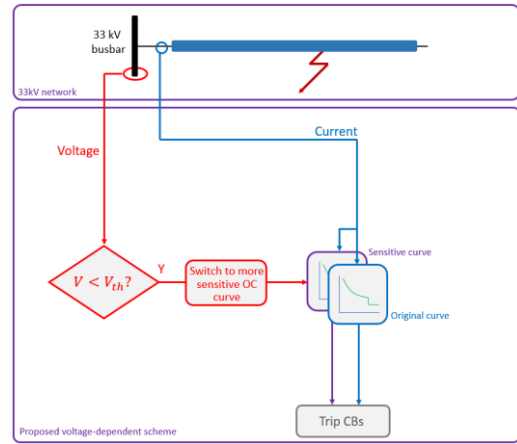


Figure 10: Operational principles of voltage-controlled relay

Figure 11 and Figure 12 present the results of a representative test case, which quantifies the performance of the voltage-controlled relay. Effectively, the feasibility of the voltage-dependent relay was assessed for a LLL solid fault occurring at 33 kV transformer incomer to Annan switchboard, during which the GFC unit is saturated (as demonstrated in Section 3 in Figure 4) and more sensitive protection settings are required (as identified in Section 5 in Figure 9).

Figure 11 depicts the voltage drop at the ‘CHAP13’ overcurrent relay point at 33kV transformer incomer to Annan switchboard. It can be seen that the voltage falls below the 85% of the nominal voltage (0.85 p.u.) and subsequently the fault is detected by the undervoltage element, and the voltage dependent relay has switched to a more sensitive IDMT setting.

The time-current characteristics for the overcurrent relay ‘CHAP13’ (shown in Figure 12) consider the settings proposed in [8] (curve indicated with red colour) and the corresponding voltage-dependent relay (curve indicated with green colour). As it can be observed, the voltage-dependent relay with the reduced pick-up current setting operates in 1.19 s after the fault occurrence, while with the standard IDMT setting, the fault is cleared 0.81 s later.

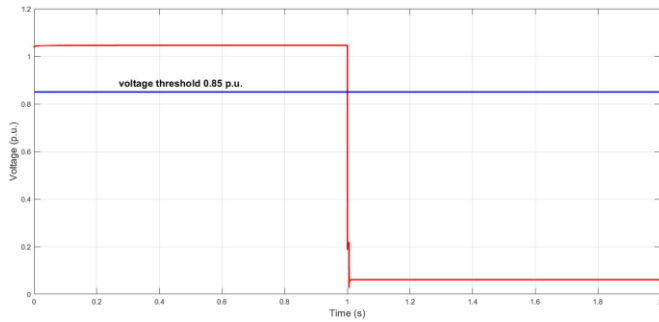


Figure 11: Voltage drop at relay point for a LLL solid fault at 33kV transformer incomer to Annan switchboard

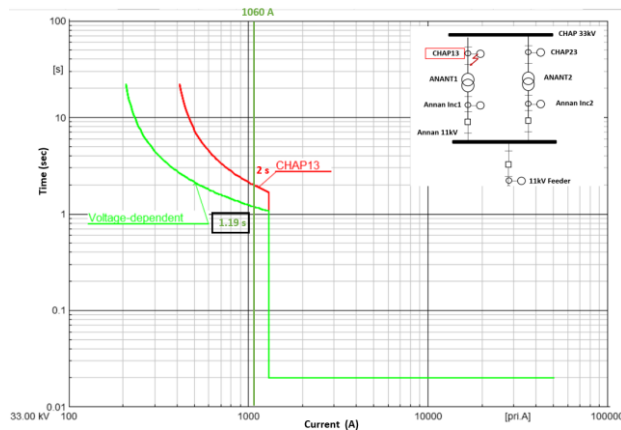


Figure 12: Time-current characteristic for an overcurrent relay and voltage-controlled overcurrent relay for a LLL solid fault at 33kV transformer incomer to Annan switchboard.

The utilization of voltage-controlled overcurrent relays does not constitute a holistic solution for the reduced fault levels. However, it can be considered as an example which illustrates that more advanced and adaptive solutions are required to tackle the challenge of the saturated fault response of GFC units. Furthermore, the presented studies can be considered as a potential research avenue for such network configurations.

7 Conclusions

In this paper, a GFC unit has been investigated as a reference generator during black-start conditions with emphasis given to the resulting fault levels at different voltage levels and its impact on the performance of overcurrent protection schemes. The simulation-based analysis and the corresponding results considered both the GFC, and a SG as reference generator, with the latter utilised for benchmarking purposes. It has been demonstrated that the fast-acting voltage support of GFC can be considered a useful feature for sustaining relatively high fault current at lower voltage levels. Specifically, at 11kV, the LLL and LG fault levels derived from the RMS short-circuit analysis with the GFC as reference generator, are higher compared to those resulting from the. Therefore, at these

voltage levels the existing protection settings provide adequate protection in terms of protection sensitivity for the case of the GFC. However, it has been revealed that the protection discrimination between the relay at the 11 kV transformer's incomer and the relay at 11 kV feeder is not always fulfilled, and therefore adjustment in the time settings may be required. At higher voltage levels (i.e 33 kV, 132 kV and 400 kV), GFC is saturated in most cases and the resulting LLL and LG fault levels are limited to the value of the nominal current. In this regard, the resulting fault clearance time is increased, and more sensitive pick-up current settings are required. Last but not least, it has been revealed that the deployment of the voltage-controlled overcurrent relay provides faster protection and hence improves the protection sensitivity, enabling the adoption of GFC units as reference generator in black-start conditions, even though this solution may face some cost related barriers as the voltage transducers are not available on all 33 kV circuits. For future research, the investigation of communication-based protection can be considered as a promising approach, as the communication-based protection schemes are widely available and cost-effective.

References

- [1] N. G. ESO, "Distributed Restart, Project Progress report -Bi-annual January-July 2019," 2019. <https://www.nationalgrideso.com/document/147516/download> (accessed Sep. 04, 2021).
- [2] N. G. ESO, "Distributed Restart-Power engineering and trials-Assessment of power engineering aspects of Black Start from DER-Part 1," 2020. <https://www.nationalgrideso.com/document/174411/download> (accessed Sep. 04, 2021).
- [3] L. Noris, J. L. Rueda, E. Rakhshani, and A. W. Korai, "Power System Black-Start and Restoration with High Share of Power-Electronic Converters," *IEEE Power Energy Soc. Gen. Meet.*, vol. 2019-Augus, pp. 1–5, 2019, doi: 10.1109/PESGM40551.2019.8973828.
- [4] M. Bahrman and P. E. Bjorklund, "The new black start: System restoration with help from voltage-sourced converters," *IEEE Power Energy Mag.*, vol. 12, no. 1, pp. 44–53, 2014, doi: 10.1109/MPE.2013.2285592.
- [5] P. Piagi and R. H. Lasseter, "Autonomous control of microgrids," *2006 IEEE Power Eng. Soc. Gen. Meet. PES*, 2006, doi: 10.1109/pes.2006.1708993.
- [6] R. H. Lasseter, Z. Chen, and D. Pattabiraman, "Grid-Forming Inverters: A Critical Asset for the Power Grid," *IEEE J. Emerg. Sel. Top. Power Electron.*, vol. 8, no. 2, pp. 925–935, 2020, doi: 10.1109/JESTPE.2019.2959271.
- [7] H. P. Beck and R. Hesse, "Virtual synchronous machine," *2007 9th Int. Conf. Electr. Power Qual. Util. EPQU*, 2007, doi: 10.1109/EPQU.2007.4424220.
- [8] ARCADIS, "Chapelcross Protection Changes Limitations Assesment-Issue B ", June 2020.